The 14th World Conference on Earthquake Engineering
October 12-17, 2008, Beijing, China

AN ANALYTICAL MODEL FOR COMPOSITE STEEL PLATE WALL

F.F. Sun[1], G.R. Liu[2] and G.Q. Li[3]

[1] *Associate Professor, Dept. of Building Engineering, Tongji University, Shanghai. China*
Email: ffsun@mail.tongji.edu.cn
[2] *Postgraduate Student, Dept. of Building Engineering, Tongji University, Shanghai. China*
[3] *Professor, Dept. of Building Engineering, Tongji University, Shanghai. China*

ABSTRACT :

A new-type of composite steel plate wall (CSPW), which consists of a steel plate sandwiched by two prefabricated concrete panels, has been recently studied. The concrete panels act only as a buckling restrainer for the steel plate by leaving a small gap between the edges of the panels and the boundary columns or beams. Thus seismic forces were resisted only by the steel plate. In this way, both cracking of a common composite wall and buckling of a common steel plate wall have been essentially avoided, ensuring excellent performance of the CSPW under seismic action. An analytical model for the CSPW – Cross-Strip Model was proposed based upon the mechanism and failure mode of CSPW. The cross sectional properties and hysteretic model for the cross strips in the model were determined with theoretical analysis. Comparison with experimental results showed that the proposed model was able to capture accurately nonlinear behavior of CSPW under monotonic and cyclic loading.

KEYWORDS: Composite steel plate wall (CSPW); Simplified model; Cross-strip model; Hysteretic model

1. INTRODUCTION

Composite steel plate wall (CSPW) is a type of lateral member for tall buildings, composed of steel plate and concrete panel connected by shear connectors (See Figure 1). The concrete panel provides out-of-plane restraint preventing premature failure of the steel plate due to buckling. Both the shear and the energy dissipating capacity of the steel plate are thus significantly improved. Moreover, the concrete panel acts also as fire proof for the steel plate. Zhao and Astaneh-Asl(2004) improved the detailing of CSPW by leaving gaps between the concrete panel and boundary members such that the lateral force is resisted only by the steel plate, protecting the concrete panel from cracking or crushing under lateral force. In this way, the protection of the concrete panel on the steel plate will not decrease during seismic actions. As continuation of the previous work of our research group – experimental and finite element analysis on CPSW, this paper intends to propose an analytical model for the CSPW.

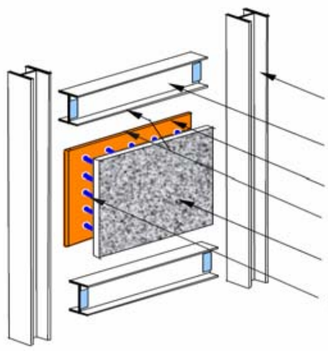

Figure 1. Main components of a CSPW.

2. MECHANISM OF CSPW

As indicated in Figure 2, thin steel plate wall(SPW) will buckle under very low compressive stress and hence resist lateral force by means of diagonal tensile action. In the case of CSPW, the steel plate will develop pure shear stress if the out-of-plane restraint provided by the concrete panel is ideal and sufficient (See Figure 3). However, according to experimental results by Tsai et al.(2006) and Gao(2007), the steel plates in CSPW exhibited diagonal tensile action similar to that of thin SPWs, as shown in Figure 4, in which residual deformation of the steel plates can be seen in diagonal directions. This is due to the gaps between the concrete panel and the boundary members, where the steel plates do not have out-of-plane restraint. Thus the diagonal residual deformations occurred in this region. Based upon the similarity between the mechanisms of the CSPW and the SPW, the strip model (Thorburn et al. 1983) suitable for the latter case will be extended to the former one.

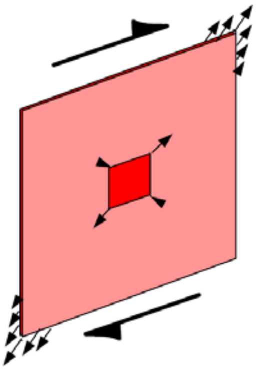

Figure 2. Stress status in a thin SPW

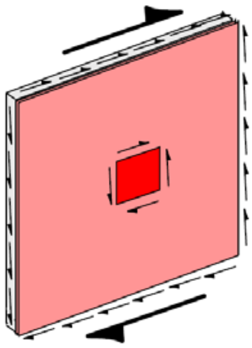

Figure 3. Ideal stress status of the steel plate in a CSPW

Figure 4. Residual deformation of the steel plate in the CSPW specimen (Gao 2007)

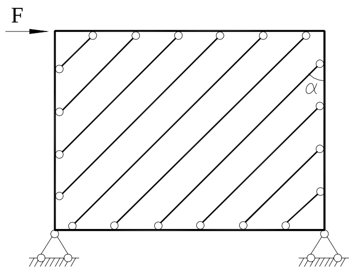

Figure 5. The strip model for SPW

In the strip model for SPW as shown in Figure 5, a group of parallel strips are employed to represent the tensile diagonal action, while in the compressive diagonal direction, no components are present as no significant compressive stress can exist due to buckling. In comparison, a large amount of compressive stresses will develop in the steel plate of a CSPW resulting from the protection of the concrete panel. Thus, a second group of parallel strips in the compressive diagonal direction will be adopted for CSPW, in addition to the tensile strips. This introduces a model named as Cross-Strip Model shown in Figure 6.

3. CROSS-STRIP MODEL

To construct a cross-strip model in Figure 6, two groups of diagonal parallel strips are defined to simulate the steel plate in a CSPW while the concrete panel will not appear in the model, as it does not resist lateral force, bearing in mind the fact that there are gaps between the concrete panel and the boundary members. The effect of the panel to restrain the out-of-plane deformation of the steel plate is modeled by allowing the compressive action of the strips. Each strip is pin-connected to the boundary members and all the strips have a same cross sectional area and are placed with equal spacing. Number of each strip group is suggested not less than 10.

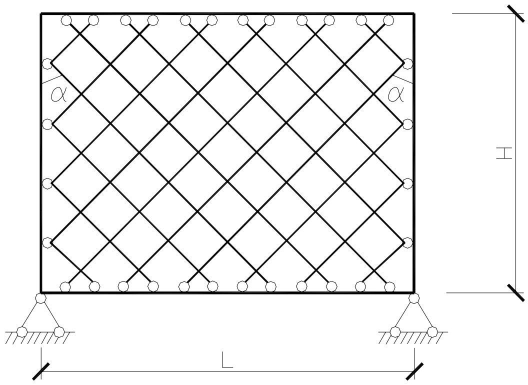

Figure 6. Cross-strip model for CSPW

3.1. Determination of strip size

The cross-sectional area of each strip, A_s, can be determined according to the spacing as follows,

$$A_S = \frac{t(L\cos\alpha + H\sin\alpha)}{n} \tag{1}$$

where t, L, H are the thickness, width and height of the steel plate, respectively; α is the angle of inclination between the strip and the vertical line; n is the number of strips in one diagonal direction.
The determination of α may make use of the formula in the theory of strip model (Thorburn et al. 1983) for SPW as follows,

$$\tan^4\alpha = \frac{1 + tL/2A_C}{1 + th\left(\frac{1}{A_b} + \frac{h^3}{360 I_C L}\right)} \tag{2}$$

where h is story height; A_c and A_b are cross-sectional area of boundary columns and boundary beams, respectively; I_c is the cross-sectional moment of inertia of boundary columns.

Driver et al.(1998) demonstrated with their experimental results that the inclination angle of SPW varied from 42° to 50°, which covers the inclination of residual plastic deformation of the steel plate of the CSPW shown in Figure 4. Numerical parametric analysis showed that the variation of the inclination angle in the above range made little influence on the shear force and story drift of SPW. Hence, α is assigned with a constant value of 45° for simplicity, resulting in a simpler formula for Equation (1) as follows,

$$A_S = \frac{\sqrt{2}}{2}\frac{t(L+H)}{n} \tag{3}$$

3.2. Determination of strip compressive strength

In the strip model for SPW, the strip is a tension-only element. When extended to the cross-strip model for CSPW, the strips in two diagonal groups are in tension and compression respectively. In the case of monotonic

loading, a tension-only element and a compression-only one can be used, while for cyclic loading case, it is better to use the same axial bar element capable of resisting both tension and compression for each strip.
The yielding and ultimate tensile stress of each strip can be simply defined as those of steel, as no interaction between the stresses in the tensile and compressive strips has been considered in the model. In this way, the compressive strength of the strips must be different from that of steel, even there is no buckling in the steel plate. This treatment may lead to errors in stress distributions in the members, but will play little effect on global behavior.
In order to determine the compressive strength, we assume both the tensile and compressive behavior are elasto-plastic. Considering the kinematic and equilibrium conditions for a hinged frame with rigid boundary columns and beams filled with a CSPW at limit state, the portion of a horizontal point load at the beam level resisted by all the tensile strips is as follows according to Berman and Bruneau (2003),

$$V_T = 0.5 f_y Lt \sin 2\alpha \tag{4}$$

which becomes

$$V_T = 0.5 f_y Lt \tag{5}$$

with the assumption of α=45°. Similarly the other portion resisted by all the compressive ones is the following

$$V_C = 0.5 f_y' Lt \, , \tag{6}$$

where f_y and f'_y are tensile and compressive strength of the strips, respectively. Thus the total capacity of the above system reads

$$V = V_T + V_C = 0.5(f_y + f_y')Lt \tag{7}$$

According to AISC Seismic Provisions(2005), the capacity of a CSPW can be evaluated as

$$V = 0.6 f_y Lt \, . \tag{8}$$

Comparing Eqs. (7) and (8) gives

$$f_y' = 0.2 f_y \tag{9}$$

which means the compressive strength of the strip can be taken as 20% of the tensile one of steel.

3.3. Selection of hysteretic rule

The experimental hysteretic behavior of CSPWs has the following high spots (See Figure 14a):
(1) the skeleton curve is bi-linear;
(2) unloading stiffness at post-yield stage is close to elastic stiffness;
(3) reloading stiffness decreases with the increase of the maximum experienced displacement;
(4) pinching effect is not significant.
Based on the above phenomena, bi-linear Clough hysteretic model shown in Figure 7 is adopted for the strips in the cross-strip model to simulate hysteretic performance of CPSWs. The hysteretic rules are as follows: initial loading follows the skeleton curve; at post-yield stage, the unloading stiffness k_3 resumes the initial stiffness k_1, i.e. k_3= k_1; reloading starts after unloading to zero stress and aims at the point at the maximum displacement ever experienced (or the yield point instead, if it has not ever reached the yield point in the reloading direction). According to Equation (9), the skeleton curve is not symmetric for the tensile and compressive branches.

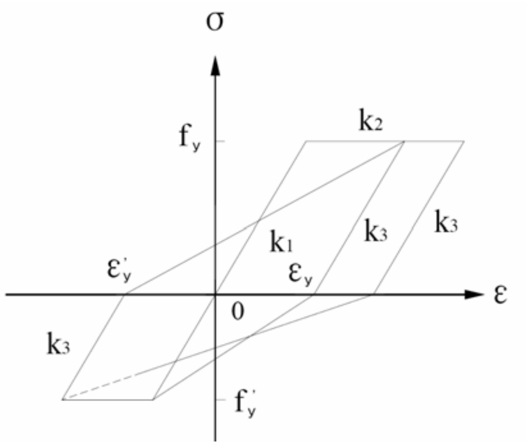

Figure 7. Bi-linear Clough hysteretic model

4. PARAMETRIC ANALYSIS AND NUMERICAL VALIDATION

4.1. Description of the experiment and numerical modeling

The experiment done by our research group is used to validate the proposed model. The specimen CW4 is modeled as only this specimen is four-sided CPSW, while others are two-sided CPSWs, i.e. only two sides of which are connected to the boundary members, beyond the scope of the proposed model. The specimen was installed in a pin-jointed frame with span of 2480mm and height of 1300mm (Figure 8). The height, width and thickness of the steel plate was 900mm, 1800mm and 2mm, respectively. The material properties of the steel plate of CW4 are listed in Table 1.

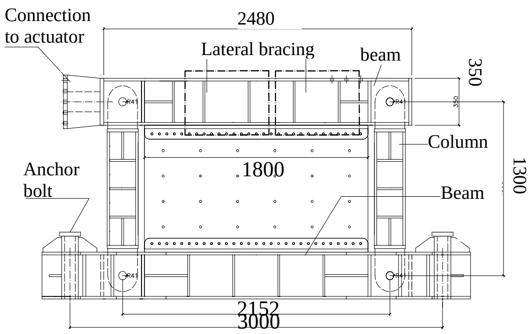

Figure 8. Test setup

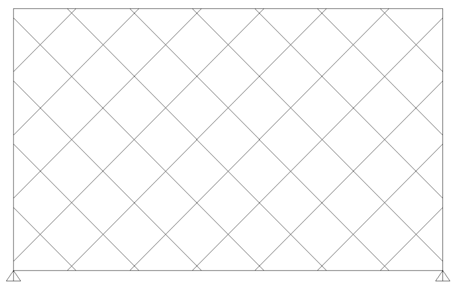
Figure 9. Model for CW4 with SAP2000

Table 1. Material properties of the steel plate of Specimen CW4

Nominal thickness	Measured thickness (mm)	Tensile strength (N/mm^2)	Yield strength (N/mm^2)	Elastic modulus (N/mm^2)	Elongation (%)
t=2mm	1.9	362.9	287.0	174499.4	36.2

Software SAP2000 is used to simulate the test. The cross-strip model for CW4 is shown in Figure 9. The boundary members are modeled with elastic beam element as they remained elastic during the test. For each strip, a fiber hinge is constructed to introduce material nonlinearity. In either diagonal direction, 10 parallel strips are constructed. The cross-sectional area of each strip is obtained with Equation (1) as follows,

$$A_S = \frac{0.707 \times 1.9 \times (1800 + 900)}{10} = 363\,\text{mm}^2 .$$

4.2. Parametric analysis on the effect of the post-yield tensile stiffness of the strips

The ratio of post-yield stiffness to initial one is chosen as the key parameter to perform parametric analysis. The yield strength of compressive strips are temporarily set as zero to avoid the effect of these strips on the parametric analysis. Five stress-strain curves with ratios of 0%, 0.5%, 1.0%, 1.5% and 2% are adopted as shown in Figure 10 and the relevant results are plotted in Figure 11. The ratio of 2% introduces an increase of horizontal force by 20% at the displacement of 30mm (approximately corresponding to an inter-storey drift of 1/50), compared with the case of 0% (i.e. elastic-ideally plastic case). In the meanwhile, the test stress-strain curve of the steel plate gives a result very close to elastic-ideally plastic case. Therefore, the stress-strain curve for the strip is proposed to be elastic-ideally elastic.

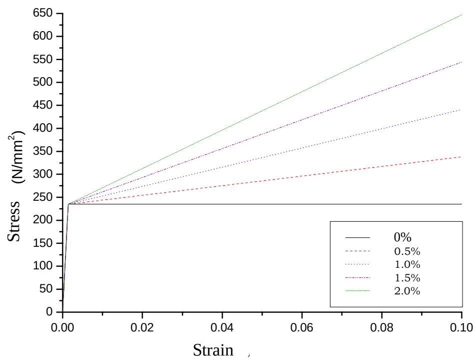

Figure 10. Variation of post-yield stiffness

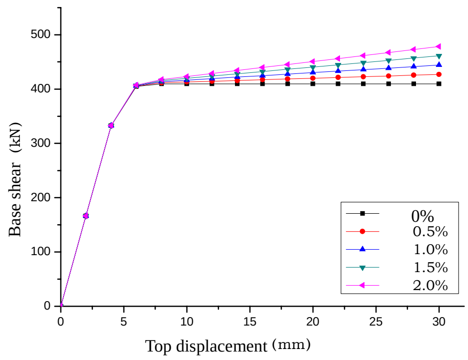

Figure 11. Effect of post-yield stiffness

4.3. Parametric analysis on the effect of the compressive strength of the strips

In order to verify Equation (9), the ratio f'_y/f_y is taken as primary parameter here. Five cases with f'_y/f_y = 0.0, 0.1, 0.2, 0.3 and 0.4 are considered. Pushover curves are shown in Figure 12 while results of initial stiffness and ultimate capacity are listed in Table 2. When f'_y/f_y = 0.0, all the compressive strips are actually inactive, thus the initial stiffness in this case is only a half of all other cases, as indicated both in Figure 12 and Table 2. According to Gao (2007), the concrete panel of CW4 contacted the fish plates after a considerably large displacement, due to out-of-plane displacement of the panel. The experimental pushover curves in Figure 12 are actually the skeleton of the original experimental hysteretic curve, which corresponds to the ultimate capacity of 792kN in brackets in Table 2. The corrected quantity of 620kN is exclusive of the contact effect (Gao 2007). As can be seen in Table 2, the ultimate capacity increases with an amount proportional to the increase in the compressive strength of the strips. The predicted ultimate capacity in the case of f'_y/f_y = 0.2 is most close to the test one, among other cases, which validates Equation (9).

Table 2. The effect of variation of compressive strength

Case	Initial stiffness (kN/mm)	Ultimate capacity (kN)
Experiment (CW4)	179	620 (794)*
f'_y/f_y = 0.0	117	500
f'_y/f_y = 0.1	234	550
f'_y/f_y = 0.2	234	600
f'_y/f_y = 0.3	234	650
f'_y/f_y = 0.4	234	700

Note: * The quantities in and out of the brackets are the measured and corrected forces, respectively.

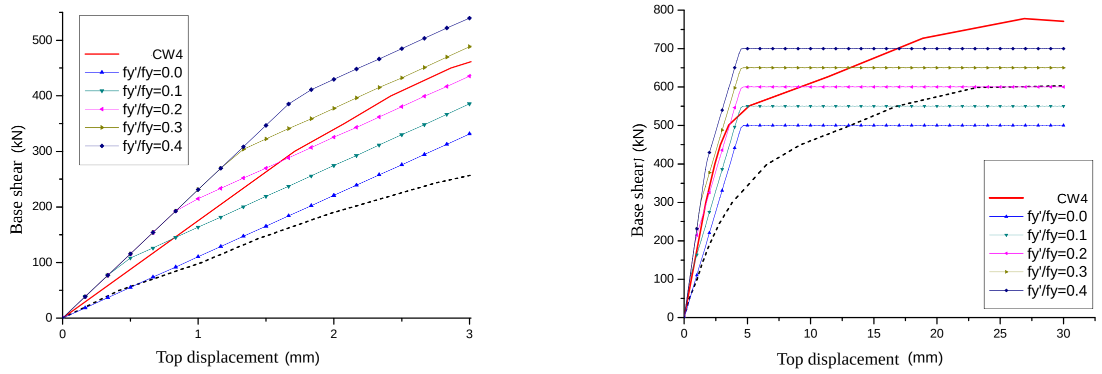

(a) (b)

Figure 12. The effect of variation of the compressive strength on pushover results

4.4. Parametric analysis on the effect of the initial compressive stiffness of the strips

As indicated by the experimental phenomenon in Figure 4, some part of the steel plate still buckled, where there was no restraint due to the gap between the concrete panel and the boundary members. The buckling must lead to a reduction in the stiffness of the specimen, which is the reason why the experimental result of initial stiffness is significantly smaller than the computational results as seen in Table 2.

In order to examine the effect of variation of initial compressive stiffness, the ratio of initial compressive stiffness, *k'*, to initial tensile one, *k*, is taken as primary parameter while the ratio f'_y/f_y is fixed as 0.2. Five cases of *k'*/*k* = 0, 1/4, 1/2, 3/4 and 1 are considered with results shown in Table 3 and Figure 13. The case of *k'*/*k* = 1/2 is most close to the experimental result. However, no conclusion can be drawn presently as little experimental results are available.

Table 3. The effect of variation of initial stiffness of compressive strips

Case	Initial stiffness (kN/mm)
Experiment (CW4)	179
k'/k=0	117
k'/k =1/4	146
k'/k =1/2	175
k'/k =3/4	205
k'/k =1	234

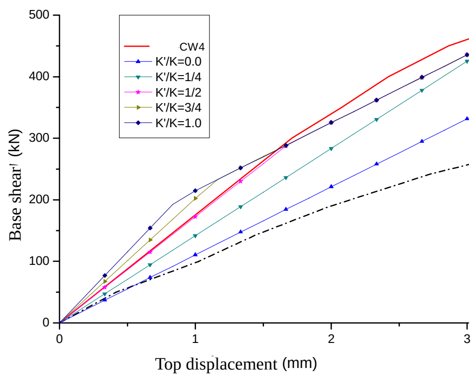

Figure 13 The effect of variation of initial stiffness of compressive strips on pushover results

4.5. Validation

With the analysis above, the bi-linear Clough hysteretic model with f'_y/f_y = 0.2 and k'/k = 1 is used to simulate hysteretic behavior of CW4. The comparison between the experimental and numerical hysteretic curves validates that the accuracy of the proposed cross-strip model is acceptable, noting that the correct experimental ultimate is 620kN, as mentioned in Table 2 .

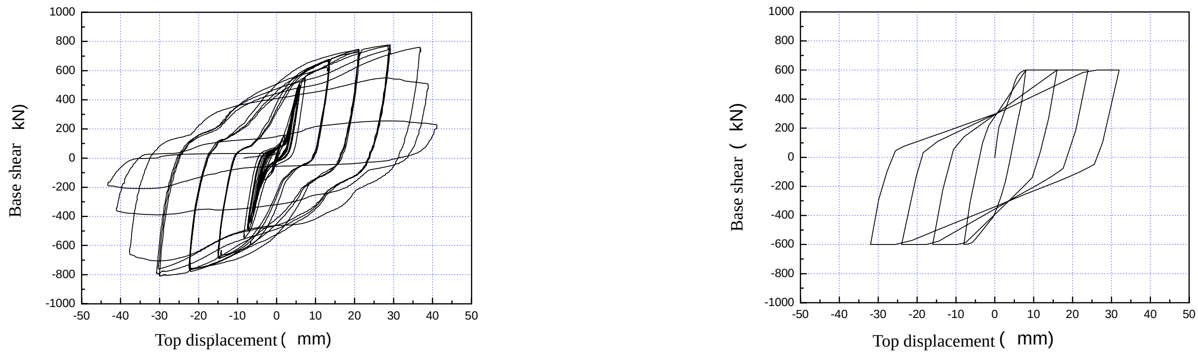

(a) Experimental (CW4) (b) Numerical

Figure 14. Validation of cross-strip model with hysteretic curves

5. CONCLUDING REMARKS

Based upon the mechanism and failure mode of CSPW, a cross-strip model was proposed and validated with experimental results. The accuracy of the proposed model needs to be further refined especially for the initial compressive stiffness of the strips, as very few tests have been done.

ACKNOWLEDGEMENT

The research is supported by Project 50408036 sponsored by National Natural Science Foundation of China, the Key Project of Chinese Ministry of Education (106069), and Key Project of China National Science & Technology Pillar Program in the Eleventh Five-year Plan Period.

REFERENCES

AISC. (2005). Seismic Provisions for Structural Steel Buildings, AISC, Chicago, USA.

Berman, J. and Bruneau, M. (2003). Plastic analysis and design of steel plate shear walls, *Journal of Structural Engineering* **129:11**, 1448-1456.

Driver R.G., Kulak G.L., Elwi A.E. and Kennedy D.J.L. (1998). FE and simplified models of steel plate shear wall. ASCE *Journal of Structure Engineering* **124:2**, 121-30.

Gao Hui. (2007). Experimental and Theoretical Studies on Composite Steel Plate Shear Walls, A dissertation submitted to Tongji University in conformity with the requirements for the degree of Master, Shanghai, China.

Tsai, K.C., Lin, Y.C. and Lin, C.H. (2006). Seismic responses and design of steel plate shear wall, The Proc. of The fourth Cross-Strait and Hong Kong Conference on Steel Structures, Shanghai, 108-116.

Thorburn, L.J., Kulak, G. L., and Montgomery, C.J. (2003). Analysis of steel plate shear walls. Structural Engineering Report. No. 107, Depart. of Civil Engrg., University of Alberta, Canada.

Zhao, Q. and A. Astaneh-Asl. (2004). Cyclic behavior of traditional and innovative composite shear walls, *Journal of Structural Engineering* **130:2**, 271-284.